BUTTERWORTH HEINEMANN

Gas. Sep. Purif. Vol. 9, No. 4, pp. 223–230, 1995

0950–4214/95 $10.00 + 0.00

0950-4214(95)00017-8

Adsorption of nitrogen, carbon monoxide, carbon dioxide and nitric oxide on molecular sieves

R.W. Triebe and F.H. Tezel*

Department of Chemical Engineering, University of Ottawa, Ottawa, Ontario, Canada

Adsorption of N_2, CO, CO_2 and NO has been studied on various molecular sieves using the gas chromatographic method to determine the potential for separation of these common atmospheric contaminants from air. The molecular sieves studied include H-Mordenite, 4A and 5A zeolite, a natural clinoptilolite and an activated carbon. Henry's law constants have been determined over a variety of temperature ranges from 243 to 473 K. Van't Hoff plots are presented for CO on all materials and for NO on all but 4A zeolite. Adsorption of CO_2 on the clinoptilolite was too strong to produce an interpretable response peak. Results of CO adsorption on 4A and 5A zeolites have been compared to and are supported by data available in the literature. Heats of adsorption for CO, NO and N_2 were determined. For CO the heats of adsorption decrease in the order of clinoptilolite > 5A zeolite > 4A zeolite > H-Mordenite > activated carbon. For adsorption of NO the heats of adsorption decrease in the order of clinoptilolite > 5A zeolite > activated carbon. Separation factors are presented for the CO/N_2 and NO/N_2 systems. The natural clinoptilolite shows most promise for the separation of CO and NO from N_2 at the temperature range 273–398 K. Diffusion coefficients for CO and N_2 on clinoptilolite between 348 and 423 K were also determined. Micropore diffusion proved to be the dominant mass transfer mechanism for both CO and N_2 in clinoptilolite under the conditions examined.

Keywords: adsorption; diffusion; clinoptilolite; N_2; CO; CO_2; NO; zeolite A; mordenite

Nomenclature

D_c	Micropore diffusivity
D_K	Knudsen diffusivity
D_L	Axial dispersion coefficient
D_M	Molecular diffusivity
D_p	Macropore diffusivity
D_0	Temperature independent diffusion constant
E_a	Diffusional activation energy
ΔH_0	Heat of adsorption at zero coverage
k	External mass transfer coefficient
K_p	Henry's law constant
K_0	Pre-exponential factor
L	Column length
R	Ideal gas constant
r_c	Micropore radius
T	Temperature
ΔU_0	Internal energy change of sorption
R_p	Macropore radius

Greek letters

μ	First moment of response peak
v	Interstitial velocity
ε	Void fraction of bed
θ	Void fraction of pellet
σ^2	Second moment of response peak
τ	Tortuosity factor

Introduction

As environmental regulations justifiably become more stringent, industry must consider economically viable means of reducing contaminant emissions to acceptable levels. Common contaminants such as CO, CO_2 and NO can presently be removed from a variety of sources via temperature swing or pressure swing adsorption (TSA or PSA). Such adsorptive separation processes have become commonplace in air bulk separations and purification applications, in favour of cryogenic distillation and gas absorption systems[1–7,28–30]. Some

* To whom correspondence should be addressed.

common separations include those of CO_x and NO_x from impure air streams at approximately ambient conditions (i.e. pollutant removal from flue gases).

A study was undertaken to screen some molecular sieves for potential separation of CO_2, CO and NO from N_2. Many synthetic zeolites have been tested for possible separation of the mentioned compounds from N_2. Haq and Ruthven studied adsorption of CO_2, CH_4, O_2 and N_2 on 4A and 5A zeolites[8,9], and Ruthven studied single and binary gas behaviour of CO, CH_4, O_2 and N_2 adsorption on 5A zeolite[14]. Tezel and Apolonatos reported on the adsorption and diffusion of CO, CH_4 and N_2 in various synthetic zeolites[18]. Adsorption of CO_2, NO, NO_2 and SO_2 on natural and synthetic mordenites and on 5A and 13X zeolites was studied by Ma and Mancel[10], and NO adsorption on a large variety of metal impregnated and untreated activated carbons and zeolites was examined by Kaneko and Inouye[16]. Anderson has taken part in studies of CO, CO_2, O_2 and N_2 on 4A zeolite[11,12], and Danner *et al.* have studied combinations of the $CO/N_2/O_2$ systems on 5A and 10X zeolites[13,34,35].

The vast amount of data available on these systems demonstrates their significance in air purification applications. However, natural zeolites have not been examined in such great detail due to industrial disadvantages, such as inconsistency of composition and cost of possible purifications and modifications. A study of adsorption of CO_2 on various natural (mordenite, ferrierite, clinoptilolite and chabazite) and synthetic zeolites showed chabazite to be a more promising adsorbent for CO_2 separation from N_2 than 4A and 5A zeolites[26]. Adsorption of CO_2, SO_2 and NH_3 on Hungarian clinoptilolites and mordenites has been studied by Kallo *et al.*[27]. An excellent review of the general structural and adsorptive properties of clinoptilolite has also been published in a series of articles[20,33,36]. These articles include experimental results comparing ion exchanged clinoptilolites to 4A zeolite for the separation of CH_4 from N_2. Again the natural zeolites showed great promise and versatility for the specified separation, and the use of clinoptilolite for the CH_4/N_2 separation has been independently supported through a PSA separation study[37]. Despite such promising results, the data available on natural zeolite adsorption properties are scarce relative to results for synthetic zeolites. The advantages of natural zeolites can only be realized through detailed studies of their adsorption properties and of the roles of various exchangeable cations in the adsorption of gases.

The molecular sieves chosen for screening studies were 4A and 5A zeolites, a synthetic H-Mordenite, a Turkish clinoptilolite and a high surface area activated carbon. The gas chromatographic method was used to determine the Henry's law constants of each system over various temperature ranges between 243 and 473 K. The separation factors (ratios of Henry's law constants) for NO, CO and CO_2 from N_2 on each molecular sieve were then calculated and compared to determine a favourable molecular sieve for separation of these common contaminants from N_2. A favourable system, that of CO and N_2 on the natural clinoptilolite, was then examined to determine the significance of various mass transfer resistances in a clinoptilolite packed column.

Experimental details

A Varian 3400 gas chromatograph (GC) equipped with a flame ionization detector (FID) and a thermal conductivity detector (TCD) was used for all experiments. Sample column specifications (for a 4A zeolite packed column) are given in *Table 1*. The column was fully contained in the GC oven for accurate temperature control. The carrier gas was preheated in a coil contained in the GC oven before passing through the sampling valve to ensure that all gases entering the column were at the designated temperature. The sampling valve introduced a 0.25 cm^3 pulse at atmospheric pressure into the preheated carrier stream. Gas sampling and the monitoring and analysis of response peaks were automatically controlled through the use of a Viewdac data acquisition system from National Instruments installed on an Akran 486 computer, ensuring accurate recording of sample introduction time.

Table 1 Column specifications

Particle mesh size	20–42
Average particle diameter	602.5 μm
Bed density	0.93 g cm^{-3}
Bed porosity	0.37
Inside diameter	0.51 cm
Bed length	10 cm

First and second moments of the response peak were calculated and the output, along with the raw data, were written into a Lotus 123 file, which allowed further data analysis and printing of the experimental results. Henry's law constants and diffusion coefficients were obtained from response curve first and second moments[15]

$$\mu = \frac{L}{v}\left[1 + \left(\frac{1-\varepsilon}{\varepsilon}\right)K_p\right] \tag{1}$$

$$\frac{\sigma^2 L}{2\mu^2 v} = \frac{D_L}{v^2} + \left(\frac{\varepsilon}{1-\varepsilon}\right) \times \left[\frac{R_p}{3k} + \frac{R_p^2}{15\theta D_p} + \frac{r_c^2}{15 D_c K_p}\right] \tag{2}$$

where it is assumed that $K_p \gg 1$ (reference 31). These equations are considered valid for a bidisperse system of spherical particles[39]. Terms on the right-hand side of Equation (2) represent contributions from axial dispersion, external film mass transfer, macropore diffusion and micropore diffusion, respectively. In order to determine the micropore (or zeolitic) diffusivity, other mass transfer contributions must be estimated. At low values of Reynolds number the external film mass transfer coefficient may be estimated as $kR_p/D_m = 1$ (reference 32). The macropore diffusion D_p may be considered a combination of molecular and Knudsen diffusion. The two diffusivities are calculated empirically[33,34] and combined according to the equation

$$\frac{1}{D_p} = \tau\left(\frac{1}{D_m} + \frac{1}{D_k}\right) \tag{3}$$

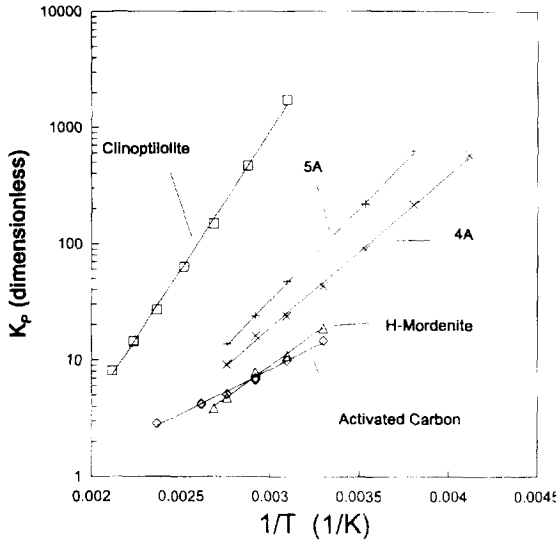

Figure 1 Dependence of Henry's law constant on temperature for CO on various zeolites

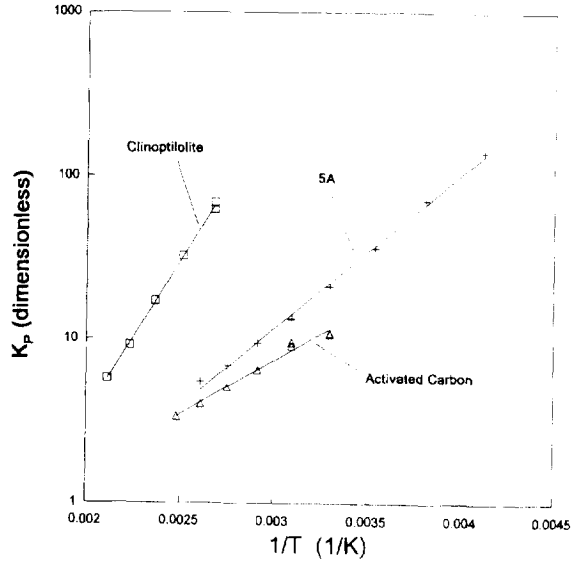

Figure 2 Dependence of Henry's law constant on temperature for NO on various zeolites

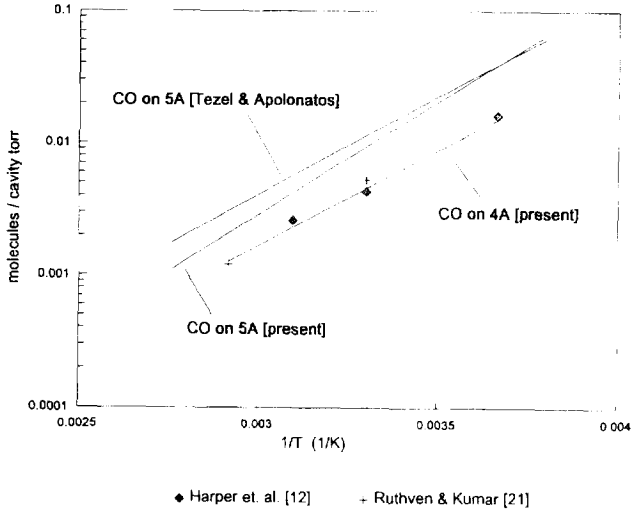

Figure 3 Comparison of experimental Henry's law constants for CO adsorption on 4A and 5A zeolites with literature values

By plotting the left-hand side of Equation (2) (the dispersion) against $1/v^2$, the axial dispersion can be determined from the slope, and the micropore resistance term may be determined from the intercept by subtracting the contributions of other resistances. Reliable values for the micropore diffusivity can only be obtained when it is the dominant mass transfer mechanism.

Gas velocities were kept low to ensure negligible pressure drop in the column. Column pressure drop was measured with a pressure gauge during all experiments and was found to be negligible. Carrier and reference gas velocities were controlled with digital flow controllers in the GC and flow rates were verified with bubble meter measurements. All tubing between sample injection and column and between column and detector was of small length and diameter to minimize the dead volume. Dead volume between sampling port and detectors was calculated at room temperature by measuring the mean of the response curve produced when a gas sample pulse was passed through the GC tubing at a known flow rate with the adsorption column removed. All experimental means of the adsorption column response curves were corrected by subtracting the corresponding dead time.

Gases used were Matheson ultra-high purity helium (99.999%), CP grade CO (99.5%), bone-dry CO_2 (99.8%) and Air Products CP grade NO (99.0%). The zeolites used were 1/8 in Linde 4A and 5A pellets, Norton Zeolon 900H-Mordenite, a natural clinoptilolite[23] and a Supelco activated carbon (with a pore size distribution between 3 and 40 Å). All synthetic zeolites were crushed and screened to produce the desired 20–42 mesh particles. The natural clinoptilolite (95% clinoptilolite crystal) was provided as 25–40 mesh particles and the activated carbon as 20–45 mesh spheres. Porosity inside the column was calculated from the bed mass and the apparent density of the zeolite particles. All molecular sieves were regenerated under helium purge first at 100°C for 2 h to remove moisture and then at 350°C for 24 h to remove any further impurities.

Results and discussion

Van't Hoff plots (semi-log plots of K_p *versus* reciprocal temperature) are given for adsorption of CO on all adsorbents screened in *Figure 1* and for NO adsorption on clinoptilolite, activated carbon and 5A zeolite in *Figure 2*. Adsorption of CO_2 on clinoptilolite was too strong to produce an interpretable response peak under the chosen experimental conditions. Since CO_2 has been thoroughly examined for determination of adsorption properties on the other common synthetic zeolites used in this study[5,6,8–12,26,27], no further CO_2 adsorption studies were conducted, and no van't Hoff plots are presented for CO_2 adsorption. Results for CO adsorption on 4A and 5A zeolite are compared with those of previous authors in *Figure 3*. *Figure 4* shows the van't Hoff plots for nitrogen adsorption on clinoptilolite and the activated carbon (present study) and on 4A and 5A zeolite (results of Haq and Ruthven[8,9]). Heats of sorption ($-\Delta H_0$) along with values of K_0 and ($-\Delta U_0$) are presented in *Table 2*. The temperature

Table 2 Parameters K_0, ΔU_0 and ΔH_0, giving the temperature dependence of K_p according to Equation (4) for the adsorbents studied, and comparison with other literature values

Sorbate	Sorbent	Reference	Temperature range (K)	K_0 (dimensionless)	$-\Delta U_0$ (kcal mol^{-1})	$-\Delta H_0$ (kcal mol^{-1})
CO	Clinoptilolite	Present	323–473	7.3×10^{-5}	10.8	11.6
	5A	Present	263–363	6.2×10^{-4}	7.2	7.8
	5A	18	303–333			6.8
	4A	Present	243–363	2.2×10^{-3}	6.0	6.6
	4A	11	193–213			5.3
	4A	12	195–323			8.0
	4A	21	305–366			6.1
	H-Mordenite	Present	303–373	5.0×10^{-3}	5.0	5.6
	H-Mordenite	18	263–363			6.0
	Activated carbon	Present	303–423	4.4×10^{-2}	3.5	4.2
NO	Clinoptilolite	Present	373–473	6.3×10^{-4}	8.6	9.4
	5A	Present	243–383	1.6×10^{-2}	4.4	5.0
	Activated carbon	Present	303–403	8.4×10^{-2}	3.0	3.7
CO_2	Activated carbon	Present	303–423	6.3×10^{-3}	5.9	6.7
N_2	Clinoptilolite	Present	323–423	1.9×10^{-4}	8.7	9.5
	Activated carbon	Present	303–403	4.2×10^{-2}	3.2	3.9

dependence of the Henry's law constant is given by the van't Hoff equation

$$K_p = K_0 e^{-\Delta U_0/RT} \tag{4}$$

K_0 and ΔU_0 are derived as the intercept and the slope of the van't Hoff plot, respectively. The value of the limiting heat of sorption can then be calculated as

$$\Delta U_0 = \Delta H_0 + RT \tag{5}$$

where R is the ideal gas constant and T is taken as the mean of the experimental temperature range.

The heats of sorptions of CO on H-Mordenite, 4A zeolite and 5A zeolite are also compared to those from previous authors in *Table 2*. Response curves for CO adsorption on activated carbon, 4A zeolite and 5A zeolite were close to Gaussian distributions. Experimental heats of sorption are in good agreement with literature values, being within 7–25% of results from various other authors for adsorption on 4A zeolite. Results on 5A and H-Mordenite are in good agreement with those of Tezel and Apolonatos (heats of adsorption within 15 and 7%, respectively)[18]. *Figure 3* shows the experimental van't Hoff plots for CO on 4A and 5A zeolites beside various literature curves and points. The magnitude of the Henry's law constants and the slopes of the curves are in excellent agreement. The experimental results therefore appear accurate when compared to other chromatographic[18,21], gravimetric[11] and volumetric[12] results.

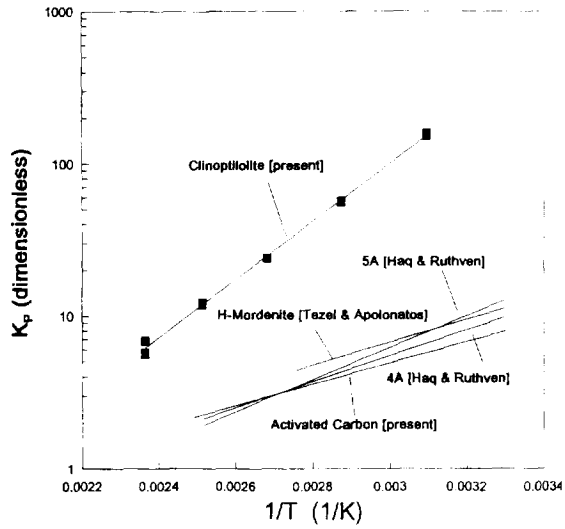

Figure 4 Dependence of Henry's law constant on temperature for N_2 on various zeolites

The CO is strongly adsorbed in both 4A and 5A zeolites, moreso in the 5A, probably due to the presence of stronger adsorption sites (bivalent Ca^{++} cations as opposed to Na^+ cations) available to interact with the strong CO dipole. The effect of bivalent cations on the adsorption of CO is well documented, and Emesh and Gay have determined that CO forms a specific complex with divalent ions in the framework of type A zeolite, having conducted experiments with ion exchanged Zn^{++}, Cd^{++}, Na^+ and Ca^{++} A zeolites. Their studies revealed an increasing capacity of A zeolite with an increase in divalent ion content due to specific complexing with the CO. However, if too many divalent ions were exchanged the adsorption capacity decreased due to the resultant inaccessibility of some of the divalent ions (now forced to occupy less accessible sites)[22]. Thus it was expected that the retention of CO in the larger pore 5A zeolite would be stronger than that in the smaller pore 4A zeolite.

Adsorption of CO in the clinoptilolite was markedly stronger than in either 4A or 5A zeolites. Henry's law constants were 50 times greater at 323 K, as is clearly shown in *Figure 1*. Reliable Henry's law constants can be difficult to obtain due to the slow diffusion in clinoptilolite. The values obtained in this study were verified by conducting experiments at a variety of gas velocities. Since the measured K_p value was the same over the entire range of velocities, the K_p values may be considered reliable. The large K_p values measured may therefore be attributed to the structure of the clinoptilolite and to the ions present. Clinoptilolite has a two-dimensional pore structure consisting of adjacent eight and ten membered ring channels interconnected by eight membered rings, allowing free movement along a plane in the zeolite.

The clinoptilolite received from Turkey has been analysed and was shown to have a Si:Al ratio of 4.25:1. The analysis of the natural ion content of the

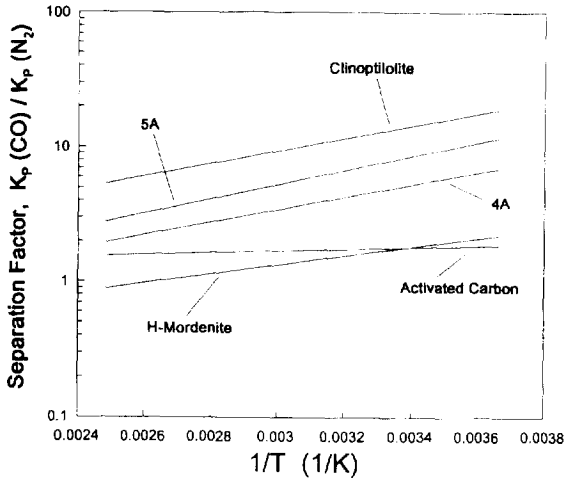

Figure 5 Adsorption equilibrium selectivities for the CO/N_2 system on various zeolites

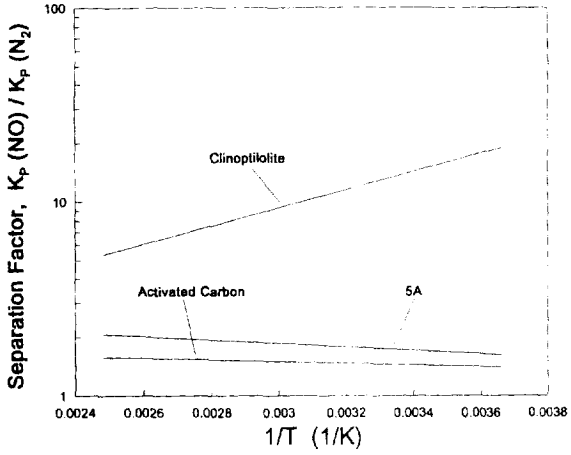

Figure 6 Adsorption equilibrium selectivities for the NO/N_2 system on various zeolites

zeolite showed Ca^{++} and K^+ as the major ions present, followed by Mg^{++} and a small amount of Na^+. Some Fe_2O_3 was also present[23]. Since the clinoptilolite is not as homogeneous as A zeolites (due to multiple pore sizes and cations) it is difficult to hypothesize precisely which effect or combination of effects caused the Henry's law constant of CO on the clinoptilolite to be so much larger than that on A zeolites and H-Mordenite. However, as previously mentioned, it is known that accessible divalent ions can form specific complexes with CO. Since Ca^{++} is present in the greatest quantity, strong adsorption of CO was expected.

Previous work[22] has shown that CO complexes with divalent cations such as Ca^{++}, Zn^{++} and Cd^{++}, and may well complex with other accessible divalent ions in a zeolite structure. Thus the Mg^{++} may also form a specific complex with the CO, leading to stronger adsorption of CO than that offered by Ca^{++} alone. It has been shown that Ca^{++} and Mg^{++} forms of clinoptilolite have higher interaction energies with N_2 than many other ionic forms[34], so the presence of the Mg^{++} ions in the pores may directly contribute to the adsorption of CO. On the other hand, the activated carbon (pore size distribution between 3 and 40 Å) offers little retention of CO due to the relatively large pore size and the lack of cations.

In order to calculate separation factors for the CO/N_2 system, the van't Hoff plot for N_2 on each molecular sieve was also required. Those on the natural clinoptilolite and the activated carbon were determined experimentally and are presented in *Figure 4*. Those for N_2 adsorption on H-Mordenite and 4A and 5A zeolites were taken from the literature. Various authors' results for N_2 adsorption on Linde 4A and 5A zeolites were examined[8,17–19]. The results chosen for calculation of the separation factors in this study were the van't Hoff equations of Haq and Ruthven[8,9] for N_2 adsorption experiments over a similar temperature range to the one in the present study. The van't Hoff equation used for description of N_2 adsorption on H-Mordenite was taken from the work of Tezel and Apolonatos[18], which was conducted in an identical fashion to the work presented here. Using these van't Hoff parameters from the literature, the separation factors (ratios of Henry's law constants) were calculated for the CO/N_2 system on 4A and 5A zeolites and compared to those determined experimentally on activated carbon and clinoptilolite in *Figure 5*. Despite the clinoptilolite's strong adsorption of N_2, it still provides the best separation factors for this system (from about 5 to 20 between 273 and 398 K), double that of 5A zeolite over the entire temperature range. Thus under ambient conditions clinoptilolite may be effective for CO removal from N_2.

The adsorption of another bipolar compound, NO (kinetic diameter of 3.17 Å), shows trends similar to those encountered with the CO (kinetic diameter of 3.76 Å). Again the compound is most strongly adsorbed in the natural clinoptilolite and least strongly adsorbed on the carbon, as displayed in *Figure 2*. Although NO (3.17 Å) is much smaller than N_2 (3.64 Å) it is more strongly adsorbed in all the molecular sieves tested. This is due to the strong diplole–cation interaction of NO as compared to the weak quadropole–cation interaction of N_2. The separation factors for NO from N_2 are presented in *Figure 6*. The results again show that the clinoptilolite gives the best separation factor between 273 and 400 K. Interestingly they show that the separation factors for NO from N_2 increase slightly with temperature. It should be noted that in typical adsorption processes for removal of NO, the NO is converted to NO_2 in the presence of O_2 and subsequently adsorbed[24,25]. Thus the separation factors for NO removal from N_2 determined in this study only apply in the complete absence of O_2. Adsorption properties of the clinoptilolite for NO_2 should be tested to fully determine the clinoptilolite's potential for separation of NO_x from common air streams.

Adsorption of CO_2 on clinoptilolite was, as mentioned previously, too strong to yield an interpretable response peak. In recording the column response for 24 h after sample pulse introduction, no discernible peak was detected. Any peak appearing beyond this time would have been uninterpretable. Previous studies of CO_2 adsorption and desorption on various clinoptilolites showed strong adsorption of CO_2 and a high degree of apparent irreversible adsorption[26]. This apparent irreversibility may explain our results, as it appears that the sample pulse of CO_2 introduced to our column either never emerged or desorbed at an extremely slow rate, even at temperatures in excess of 100 °C. Isotherms for CO_2 adsorption on the Turkish

clinoptilolite have been determined by direct measurement methods and strong adsorption of CO_2 on the clinoptilolite was apparent[23]; but these results offer no insight into the possible irreversible adsorption of CO_2.

Since the clinoptilolite showed potential for separation of CO from N_2, it was decided to study the kinetic characteristics of CO and N_2 adsorption on clinoptilolite. Response peaks for adsorption of CO and N_2 on clinoptilolite were analysed at various temperatures. Plots of total dispersion ($\sigma^2 L/2\mu^2 v$) *versus* temperature were produced and are presented in *Figure 7*. For both gases the dispersion is strongly dependent on temperature. Since all terms other than micropore diffusion on the right-hand side of Equation (2) are weak functions of temperature, this result suggests that the micropore diffusion is a significant resistance over this temperature range and that it may be measured by gas chromatographic methods.

It should be noted here that the micropore diffusivity calculated in this way incorporates not only the resistance of free diffusion through the pores, but represents a more complex transport resistance (i.e. including specific sorbate–sorbent interactions). Thus the micropore diffusivity calculated here well describes the effective diffusivity of the sorbate through the micropores, but does not define the specific mechanism or mechanisms which lead to these reported values of this effective micropore diffusivity. The parameter D_c will continue to be referred to as micropore diffusivity, and it is understood that this title does not refer to the mechanism, but rather to the total effective transport resistance in the micropores.

Experiments to determine the diffusivities of both gases were then conducted at four temperatures, varying the gas velocity at each temperature. The results, plotted as total dispersion *versus* $1/v^2$, are shown in *Figures 8* and *9* for CO and N_2, respectively. Only the high and low temperature data are shown for each gas. As the lines are so similar, this was done to avoid crowding. The slope of these plots represents the axial dispersion, and the intercept represents the other combined mass transfer resistances [Equation (2)]. In estimating the macropore diffusivity, the effects of both

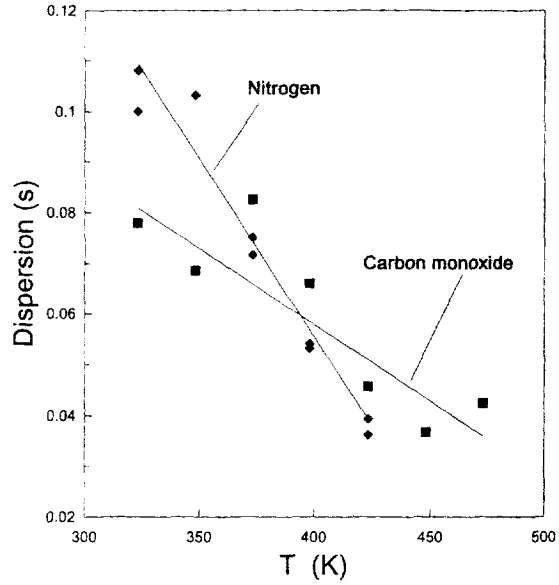

Figure 7 Dependence of dispersion on temperature for CO and N_2 on clinoptilolite

Knudsen and molecular diffusivity were taken into account, using conservative values for the tortuosity factor. Experimental values of macropore tortuosities in various zeolites range from 1.7 to 6[29,30]. Exact values of macropore diffusion resistance were not of interest in this study. Rather, it was desired to see if the macropore diffusion resistance was significant compared to the micropore resistance.

A tortuosity of 6 was chosen for the calculation, thereby estimating the maximum contribution of the macropore diffusion resistance. The resulting macropore diffusion resistances are presented with experimentally measured values of the total mass transfer resistance [$\sigma^2 L(1-\varepsilon)/2\mu^2 v\varepsilon$] and the axial dispersion, along with empirically determined values of external mass transfer resistance in *Table 3*. Since the estimated maximum macropore diffusion resistance consisted of only 2–4% of the total resistance, and the contribution from external mass transfer was considerably less

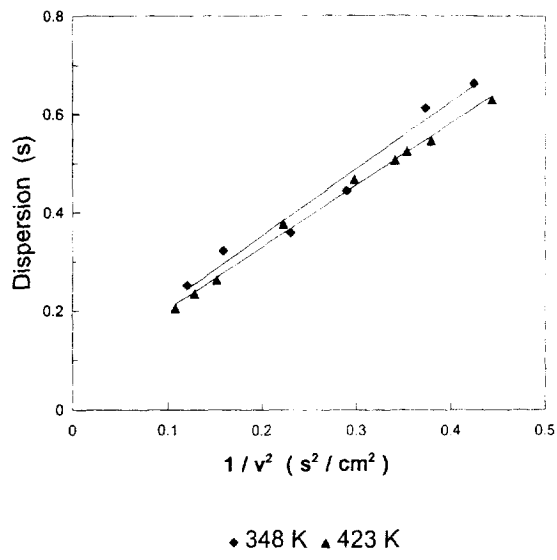

Figure 8 Dispersion *versus* ($1/v^2$) for CO/clinoptilolite system

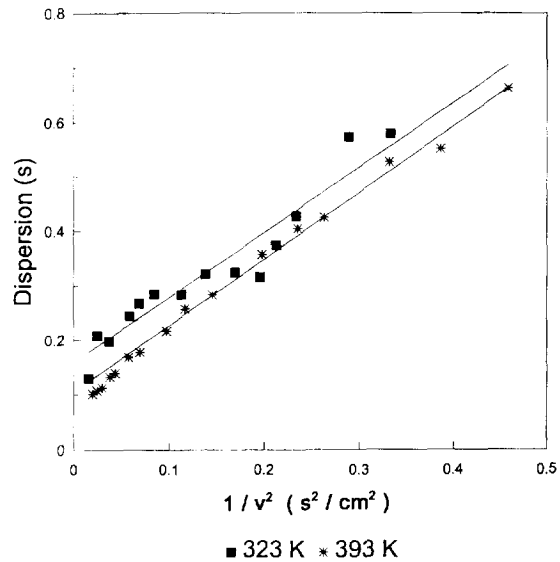

Figure 9 Dispersion *versus* ($1/v^2$) for N_2/clinoptilolite system

Table 3 Contributions of different mass transfer resistances to total dispersion for CO and N_2 in clinoptilolite

Temperature (K)	D_L/v^2 (s)	$R_p^2/3D_M$ (s)	$R_p^2/15\theta D_p$ (s)	$\sigma^2 L(1-\varepsilon)/2\mu^2 v\varepsilon$ (s)
CO at 348	1.36	11.8×10^{-4}	5.05×10^{-3}	0.14
CO at 373	1.02	10.5×10^{-4}	4.60×10^{-3}	0.15
CO at 398	1.27	9.42×10^{-4}	4.22×10^{-3}	0.10
CO at 423	1.26	8.51×10^{-4}	3.89×10^{-3}	0.13
N_2 at 323	1.21	13.5×10^{-4}	5.65×10^{-3}	0.27
N_2 at 353	1.06	11.7×10^{-4}	5.00×10^{-3}	0.23
N_2 at 373	0.998	10.6×10^{-4}	4.64×10^{-3}	0.17
N_2 at 393	1.22	9.76×10^{-4}	4.33×10^{-3}	0.18

($\approx$1% of the total resistance), then the micropore diffusional resistance must be dominant under the conditions considered. The values of the micropore diffusivity (expressed as D_c/r_c^2) were then calculated from the intercepts of the dispersion *versus* $1/v^2$ plots and are presented in *Figure 10*. The clinoptilolite crystal size was reported to be from 1 to 5 μm (reference 23). No accurate size distribution or mean crystal size was reported, so all values were expressed as D_c/r_c^2.

The temperature dependence of the micropore diffusivity may be expressed by an Arrhenius type equation

$$\frac{D_c}{r_c^2} = \frac{D_0}{r_c^2}\exp\left(\frac{-E_a}{RT}\right) \qquad (6)$$

The resulting values of the parameters D_0/r_c^2 and E_a are presented in *Table 4*. The lines have similar slopes, with diffusivities increasing with temperature as expected. The diffusivity of N_2 is three times higher than that of CO over the entire temperature range. It is clear that the natural form of the Turkish clinoptilolite used has potential for separation of N_2 and CO. It should be noted that in recent studies performed by Ackley and Yang[20,33,36] the effect of ion exchange on adsorption of N_2 and CH_4 was examined. Their results demonstrated the versatility offered by the various ionic forms of clinoptilolite. It is possible that the Turkish clinoptilolite could also be modified to improve N_2/CO separation factors. The effect of ion exchange in the Turkish clinoptilolite on CO_2 adsorption has been studied and, as in Ackley and Yang's results, the effect was found to be quite pronounced[23]. Different ionic forms of the same clinoptilolite could strongly adsorb or completely reject the CO_2. Therefore it seems reasonable to continue studying the most abundant natural zeolite, clinoptilolite, for gas separations, as the versatility and effectiveness offered by the various ion exchanged forms of clinoptilolite may outweigh the industrial disadvantages suffered by natural zeolites.

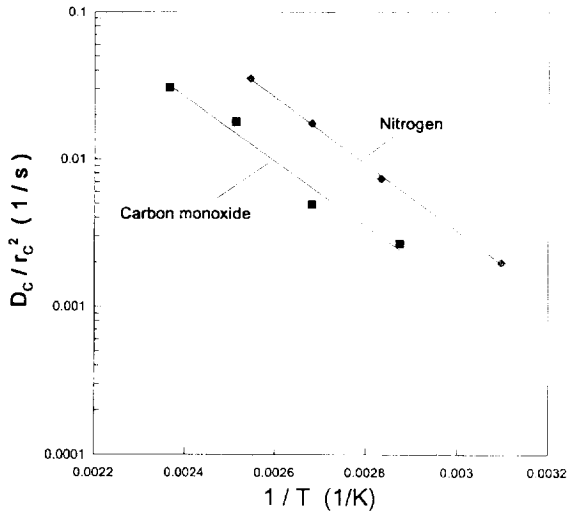

Figure 10 Temperature dependence of micropore diffusivity for N_2 and CO on clinoptilolite

Table 4 Parameters D_0/r_c^2 *and* E_a according to Equation (6) for N_2 and CO adsorption on clinoptilolite

Sorbate	Temperature range (K)	D_0/r_c^2 (s^{-1})	E_a (kcal mol^{-1})
CO	348–423	4.60×10^3	10.0
N_2	323–393	2.01×10^4	10.4

Conclusions

1 The clinoptilolite yielded the strongest adsorption of CO, NO and N_2 between 323 and 473 K as compared to 4A and 5A zeolites, H-Mordenite, and an activated carbon.
2 CO_2 was strongly and possibly irreversibly adsorbed on the clinoptilolite.
3 The clinoptilolite yielded CO/N_2 and NO/N_2 separation factors higher than those provided by any of the other sieves tested over the entire experimental range.
4 The experimental van't Hoff plots for CO adsorption on 4A and 5A zeolites are in excellent agreement with those of other authors.
5 Micropore diffusion is the dominant mass transfer mechanism for both CO and N_2 in clinoptilolite.
6 Diffusion of N_2 in the clinoptilolite was three times greater than that of CO under the conditions examined.
7 The proven versatility of ion exchanged clinoptilolites indicates that the clinoptilolite structure may offer even better separation in an ion exchanged form.

Acknowledgement

Financial support from the Natural Sciences and Engineering Research Council (NSERC) of Canada is gratefully acknowledged.

References

1 **Labrousse, M.** Non-cryogenics oxygen production: largest in Europe, paper presented at Int Symp on Gas Sep Techniques, Antwerp, Belgium (1989)

2 **Thorogood, R.M., Bennet, D.L., Allam, R.J. and Prentice, A.L.** Air separation process using packed columns for O_2 and Ar recovery *US Patent 4 871 382* (1989)

3 **Lee, H. and Stahl, D.E.** Oxygen rich gas from air by pressure swing adsorption process *AIChE Symp Ser No. 134* (1973) **69** 1–8

4 **Kasuya, F. and Tsuji, T.** High purity CO gas separation by pressure swing adsorption *Gas Sep Purif* (1991) **5** 242–246

5 **Giacobbe, F.W.** Use of physical adsorption to facilitate the production of high purity oxygen *Gas Sep Purif* (1989) **3** 133–138

6 **Giacobbe, F.W.** Adsorption of very low level carbon dioxide impurities in oxygen on a 13X molecular sieve *Gas Sep Purif* (1991) **5** 16–19

7 **Breck, D.W.** *Zeolite Molecular Sieves: Structure, Chemistry and Use* John Wiley & Sons Inc., New York, USA (1973)

8 **Haq, N. and Ruthven, D.M.** A chromatographic study of sorption and diffusion in 5A zeolite *J Coll Interface Sci* (1986) **112** 164–169

9 **Haq, N. and Ruthven, D.M.** Chromatographic study of sorption and diffusion in 4A zeolite *J Coll Interface Sci* (1986) **112** 154–163

10 **Ma, H.M. and Mancel, C.** Diffusion studies of CO_2, NO, NO_2, and SO_2 on molecular sieve zeolites by gas chromatography *AIChE J* (1972) **18** 1148–1153

11 **Eagan, J.D. and Anderson, R.B.** Kinetics and equilibrium of adsorption on 4A zeolite *J Coll Interface Sci* (1975) **50** 419–433

12 **Harper, R.J. Stifel, G.R. and Anderson, R.B.** Adsorption of gases on 4A synthetic zeolite *Can J Chem* (1969) **47** 4661–4669

13 **Danner, R.P. and Wenzel, L.A.** Adsorption of carbon monoxide nitrogen, carbon monoxide–oxygen and oxygen–nitrogen mixtures on synthetic zeolites *AIChE J* (1969) **15** 515–520

14 **Ruthven, D.M.** Sorption of oxygen, nitrogen, carbon monoxide, methane, and binary mixtures of these gases in a 5A molecular sieve. *AIChE J* (1976) **22** 753–759

15 **Sarma, P.N. and Haynes, H.W.** Application of gas chromatography to measurements of diffusion in zeolites *Adv Chem Ser* (1974) **133** 205–217

16 **Kaneko, K. and Inouye, K.** Adsorption activity of NO on iron oxide-dispersed porous materials *Adv Sci Techn* (1988) 239–250

17 **Miller, G.W., Knaebel, K.S. and Ikels, K.G.** Equilibria of nitrogen, oxygen, argon, and air in molecular sieve 5A *AIChE J* (1987) **33** 194–201

18 **Tezel, F.H. and Apolonatos, G.** Chromatographic study of adsorption for N_2, CO and CH_4 in molecular sieve zeolites *Gas Sep Purif* (1993) **7** 11–17

19 **Yucel, H. and Ruthven, D.M.** Diffusion in 4A zeolite *JCS Faraday I* (1980) **76** 60–70

20 **Ackley, M.W., Giese, R.F. and Yang, R.T.** Clinoptilolite: untapped potential for kinetic gas separations *Zeolites* (1992) **12** 780–788

21 **Ruthven, D.M. and Kumar, R.** An experimental study of single-component and binary adsorption equilibria by a chromatographic method *Ind Eng Chem Fundam* (1980) **19** 27–32

22 **Emesh, I.T.A. and Gay, I.D.** Adsorption and ^{13}C n.m.r. studies of ethene, ethane and carbon monoxide on Zn- and Cd-exchanged A zeolites *J Chem Tech Biotechnol* (1985) **35A** 115–120

23 **Sirkecioglu, A., Altay, Y. and Erdem-Senatalar, A.** manuscript in preparation

24 **Joithe, W., Bell, A.T. and Lynn, S.** Removal and recovery of NO_x from nitric acid plant tail gas by adsorption on molecular sieves *Ind Eng Chem Proc Des Dev* (1972) **11** 434–439

25 **Sundaresan, B.B., Harding, C.I., May, F.P. and Hendrickson, E.R.** Adsorption of nitrogen oxides from waste gas *Environ Sci Techn* (1967) **1** 151–156

26 **Inui, T., Okugawa, Y. and Yasuda, M.** Relationship between properties of various zeolites and their CO_2-adsorption behaviours in pressure swing adsorption operation *Ind Eng Chem Res* (1988) **27** 1103–1109

27 **Kallo, D., Papp, J. and Valyon, J.** Adsorption and catalytic properties of sedimentary clinoptilolite and mordenite from the Tokaj Hills, Hungary *Zeolites* (1982) **2** 13–16

28 **Michele, H.** Purification of flue gases by dry sorbents – possibilities and limits *Int Chem Eng* (1987) **27** 183–187

29 **Yang, R.T.** *Gas Separation by Adsorption Processes* Butterworths, Boston, MA, USA (1987)

30 **Ruthven, D.M.** *Principles of Adsorption and Adsorption Processes* John Wiley & Sons Inc., New York, USA (1984)

31 **Shah, D.B. and Ruthven, D.M.** Measurement of zeolitic diffusivities and equilibrium isotherms by chromatography *AIChE J* (1977) **23** 804–809

32 **Schneider, P. and Smith, J.M.** Adsorption rate constants from chromatography AIChE J (1968) **14** 762–771

33 **Ackley, M.W. and Yang, R.T.** Adsorption characteristics of high-exchange clinoptilolites *Ind Eng Chem Res* (1991) **30** 2523–2530

34 **Dorfman, L.R. and Danner, R.P.** Equilibrium adsorption of nitrogen–oxygen–carbon monoxide mixtures on molecular seive type 10X *AIChE J Symp Ser No 152* (1979) **71** 30–39

35 **Nolan, J.T., McKeehan, T.W. and Danner, R.P.** Equilibrium adsorption of oxygen, nitrogen, carbon monoxide, and their binary mixtures on molecular sieve type 10X *J Chem Eng Data* (1981) **26** 112–115

36 **Ackley, M.W. and Yang, R.T.** Diffusion in ion exchanged clinoptilolites *AIChE J* (1991) **37** 1645–1656

37 **Frankiewicz, T.C. and Donnely, R.G.** Methane/nitrogen gas separation over the zeolite clinoptilolite by the selective adsorption of nitrogen, in *Industrial Gas Separations* (Eds Whyte, Jr, T.E. *et al.*) ACS, Washington, DC, USA (1983)

38 **Tsitsishvili, G.V. and Andronikashvili, T.G., Thaddens, E. Y., Carmen, M. and Wagener, E. H.** *Natural Zeolites* Ellis Horwood, New York, USA (1992)

39 **Haynes, H.W. and Sarma, P.N.** A model for the application of gas chromatography to measurements in bidisperse structured catalysts *AIChE J* (1973) **19**(5) 1043–1046